Supplemental Material for

Mesoporous Zirconia Coating for Sensing Applications using Attenuated Total Reflection Fourier Transform Infrared Spectroscopy

Dominik Wacht[1], Mauro David[2], Borislav Hinkov[2], Hermann Detz[2,3], Andreas Schwaighofer[1], Bettina Baumgartner[1] and Bernhard Lendl[1*]

[1]Research Division of Environmental Analytics, Process Analytics, Institute of Chemical Technologies and Analytics, Technische Universität Wien, Getreidemarkt 9, 1060 Vienna, Austria

[2]Institute of Solid State Electronics & Center for Micro- and Nanostructures, Technische Universität (TU) Wien, 1040 Vienna, Austria

[3]Central European Institute of Technology, Brno University of Technology, Brno, Czech Republic

*E-mail: bernhard.lendl@tuwien.ac.at

Influence of the Aging Parameters

The X-ray diffraction (XRD) patterns of Si wafers used for the evaluation of the aging process are displayed in FIGURE S1.

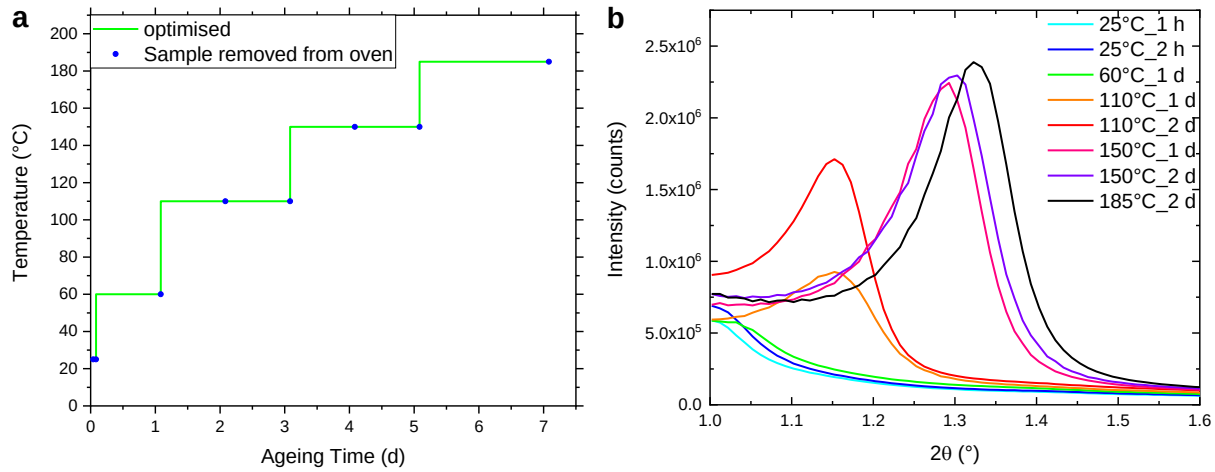

Figure S1. (a) Optimized aging process with markers representing samples, which were removed from the oven at the displayed aging time and temperature; (b) the corresponding XRD patterns.

Keeping the coating at 60 °C for 2 d reduced the intensity of the diffraction peak. A new optimized aging process as seen in FIGURE S1 was investigated. As none of the temperature steps shows a visible decrease in diffraction peak intensity associated with the mesostructure, the aging process was optimized.

Influence of the Relative Humidity During Spin Coating

The influence of the relative humidity (RH) during spin coating is displayed in FIGURE S2.

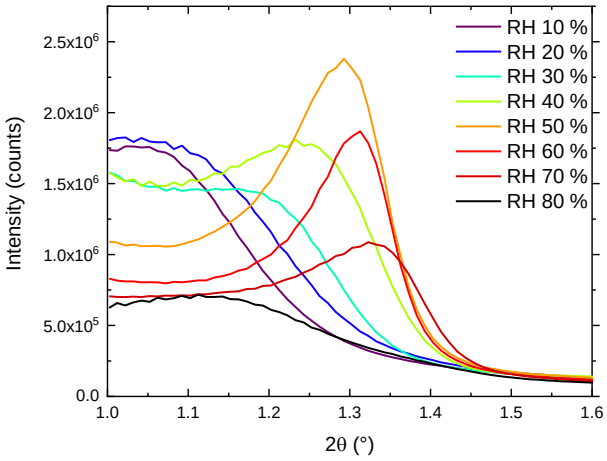

Figure S2. XRD patterns of the coatings spin coated at different RHs following the aging process.

FT-IR Absorbance Spectra After the Aging Process

FIGURE S3 displays FT-IR absorbance spectra of the ZrO_2 coating on Si-ATR crystals after the aging process. Bands at 2966 cm^{-1} and from 1450 cm^{-1} to 1250 cm^{-1} are associated with CH stretching and bending vibrations, respectively. A band at 1083 cm^{-1} is a prominent feature in the IR spectrum of polyether corresponding to the COC stretching vibration.[1]

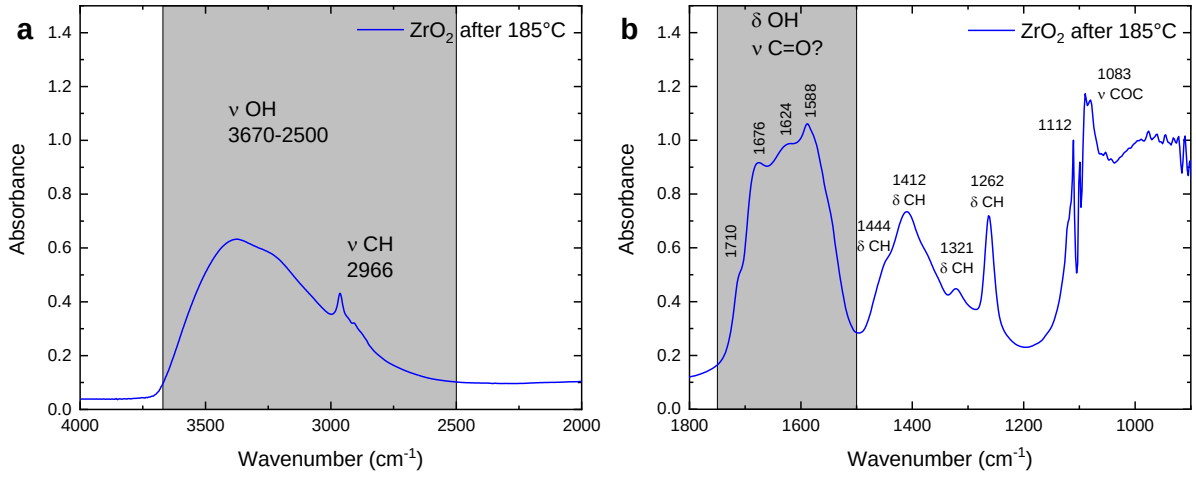

Figure S3. FT-IR absorbance spectra of coated Si-ATR crystals after the aging process: (a) from 4000 cm^{-1} to 2000 cm^{-1} and (b) from 1800 cm^{-1} to 900 cm^{-1}.

1. G. Socrates. Infrared and Raman Characteristic Group Frequencies: Tables and Charts. Chichester; New York: Wiley. 2nd ed. 1994; p viii.

Thermal Stability Studies

A second temperature stability study of the mesoporous ZrO_2 coating was also conducted. To this purpose, the coating was calcined at 500 °C with a ramp of 1 °C min^{-1} for different periods of time. Small-angle and wide-angle XRD patterns were collected after the calcination process. The wide-angle XRD patterns of ZrO_2 coatings after calcination for different periods of time are displayed in FIGURE S4, and for comparison, the wide-angle XRD pattern of a blank Si wafer is shown in FIGURE S5. Wide-angle XRD patterns after calcination showed no diffraction peaks associated with crystalline ZrO_2.

The small-angle XRD patterns in Figure S6 show a decrease in diffraction peak intensity and a shift to higher diffraction angles upon increasing the calcination time. However, even after 24 h a diffraction peak associated with the mesostructure is clearly visible.

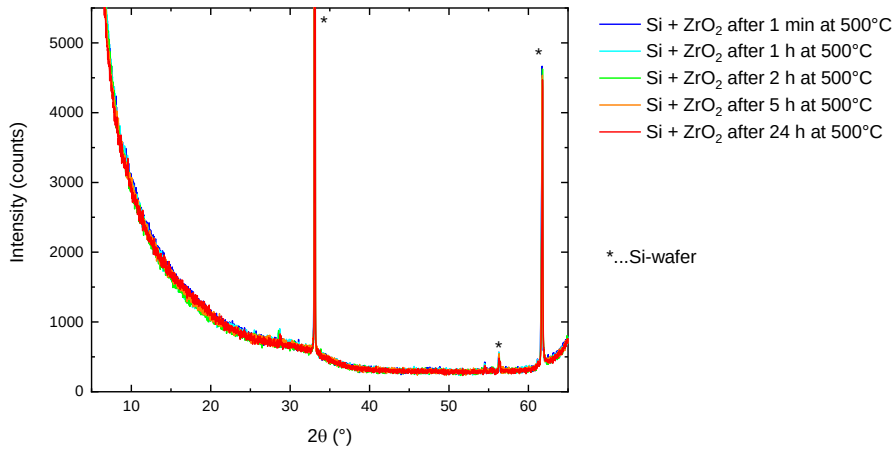

Figure S4. Wide-angle XRD patterns of the ZrO_2 coating after calcination for 1 min, 1 h, 2 h, 5 h, and 24 h.

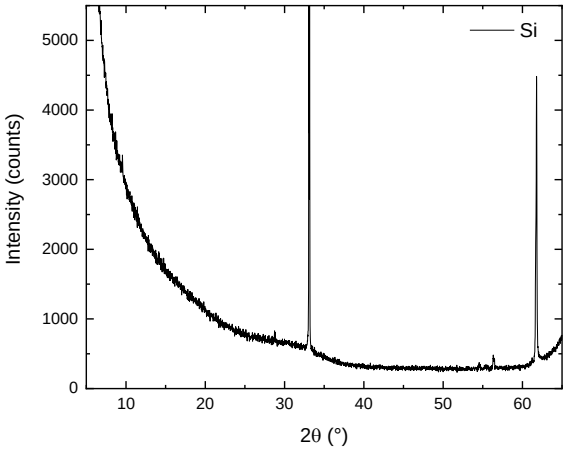

Figure S5. Wide-angle XRD pattern of an uncoated Si-wafer.

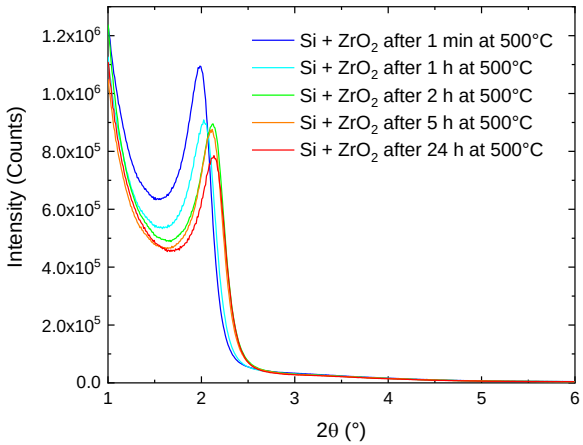

Figure S6. Small-angle XRD patterns of mesoporous ZrO_2 coatings calcined at 500 °C for 1 min, 1 h, 2 h, 5 h, and 24 h after the aging process.

Chemical Stability Studies

Microscopic images, small-angle XRD patterns, and FT-IR absorbance spectra of SiO_2-coated Si-ATR crystals before and after placing the crystal in aqueous 0.01 M NaOH solution for 12 h are displayed in Figure S7. The removal of the SiO_2 coating is evident from the missing diffraction peaks, absorbance bands, and lack of visible structure and coloration after NaOH treatment.

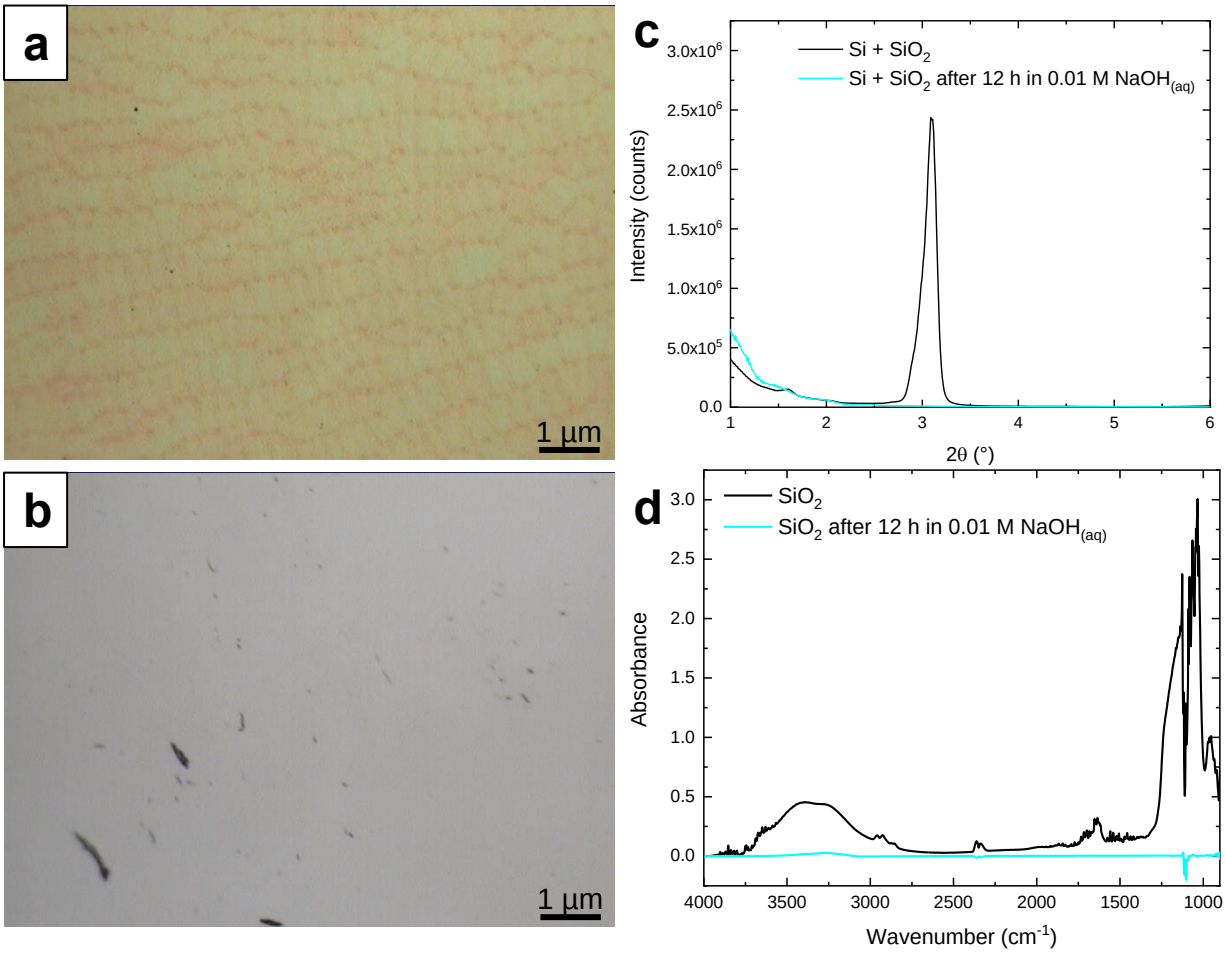

Figure S7. Microscopic images of SiO_2-coated Si-ATR crystals (**a**) before and (**b**) after placing the coating in 0.01 M $NaOH_{(aq)}$ solution. (**c**) XRD patterns and (**d**) FT-IR absorbance spectra before and after placing the coating in 0.01 M $NaOH_{(aq)}$ solution.

Refractive Index Measurements

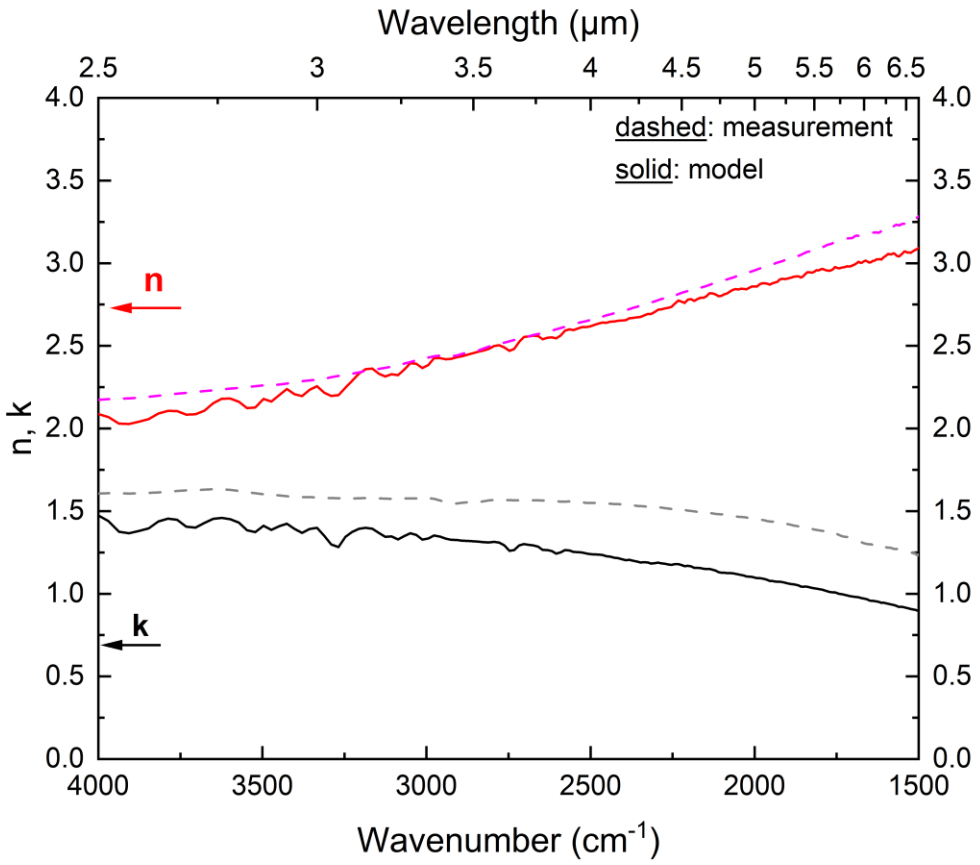

Figure S8. Wavelength-dependent MIR refractive indices of the pristine ZrO_2-coating on Si substrate. A refractive index of 1.72 at 2300 cm^{-1} for the ZrO_2-coating was extracted from the optical response of the combined Si/ZrO_2 stack.

Spectral Transmittance of ZrO_2

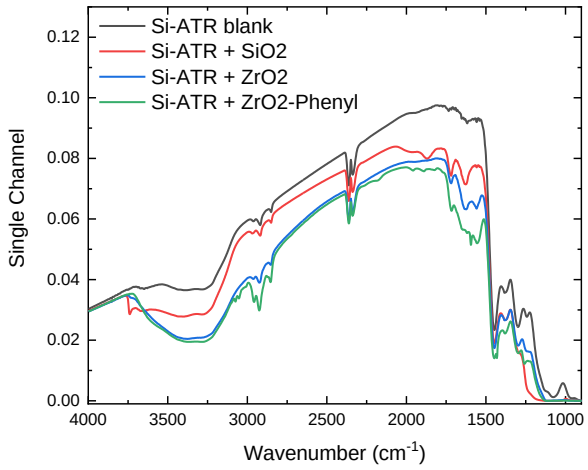

Figure S9. Single channel spectra of different mesoporous films.

Influence of the Flow Rate on the Adsorption of Benzonitrile Solutions

The enrichment of an aqueous 100 mg L^{-1} benzonitrile solution using the phenyl-modified ZrO_2 coating is displayed in Figure S9. The calculated areas of the CN band depending on the flow rate show that the obtained value is independent of the flow rate. Only the velocity of the adsorption and desorption changes with the flow rate.

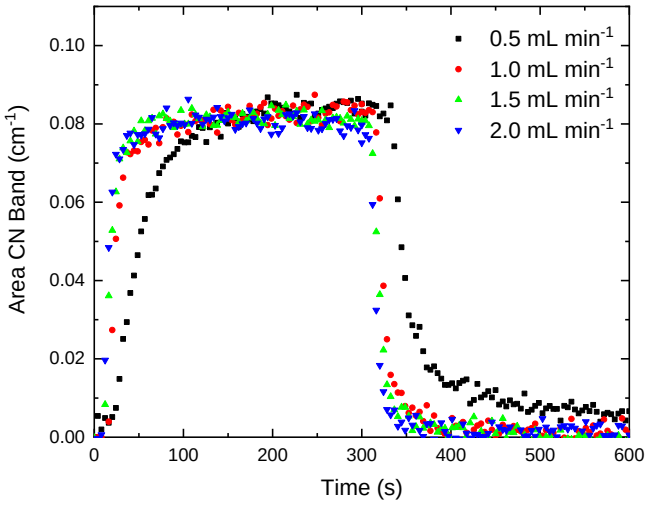

Figure S10. Flow rate dependence of the adsorption and desorption of 100 mg L^{-1} benzonitrile in water using the phenyl-modified ZrO_2 coating.